Crystalline-to-amorphous phase transformation in ion-irradiated GaAs

R. A. Brown

Research School of Physical Sciences and Engineering, Australian National University, Canberra, A. C. T. 0200, Australia and School of Physics, University of Melbourne, Parkville 3052, Australia

J. S. Williams

Research School of Physical Sciences and Engineering, Australian National University, Canberra, A. C. T. 0200, Australia

(Received 28 December 1999; revised manuscript received 24 May 2001; published 19 September 2001)

The crystalline-to-amorphous phase transformation in GaAs irradiated with B, C, O, Si, Ar, or Ge ions has been investigated by transmission electron microscopy and Rutherford backscattering with ion channeling. The critical relationships between ion flux and substrate temperature which define the threshold conditions for amorphization in GaAs by irradiation with various ions have been measured. The amorphous phase forms over a wide range of irradiation conditions by a collapselike nucleation process when a critical free energy is exceeded. The threshold conditions for nucleation are shown to be thermally activated, with a single activation energy of 0.9 ± 0.1 eV, independent of ion species, energy, or fluence. However, despite the independence of the measured activation energy on ion species, the critical temperature for amorphization does not scale linearly with the rate of energy deposition or displacement density, indicating that details of the collision cascade which influence defect quenching, trapping, clustering and annihilation processes determine the pathway to amorphization. We speculate that this results from the difficulty of nucleating the amorphous phase at temperatures where defects are highly mobile, and that nucleation occurs locally at stable defect complexes which are formed more readily in the dense collision cascades created by heavier ions.

DOI: 10.1103/PhysRevB.64.155202 PACS number(s): 61.80.Jh, 61.72.Cc, 61.72.Vv, 61.72.Yx

I. INTRODUCTION

The structural damage produced in crystalline semiconductors by ion irradiation at temperatures above 0 K is affected by the flux of the irradiating ions, with the overall degree of damage typically increasing with increasing ion flux.[1] Radiation damage will increase with increasing ion flux whenever residual defects from the collision cascade created by a single ion have not stabilized when they encounter additional defects from a subsequent ion impact, and the new defect(s) thus formed is (are) more stable than the individual components. In GaAs, the overall degree of structural damage, as measured by Rutherford backscattering (RBS) with ion channeling, has been shown to have a power law dependence on N or Si ion flux at low damage levels near room temperature.[2,3] It is surprising how often ion flux is overlooked in the literature, with the majority of published reports neglecting to consider it as a relevant factor. Given the knowledge that damage in GaAs is typically sensitive to both substrate temperature and ion flux,[4] it seems remarkable that the relationship between these key parameters has never been investigated.

Recently, we demonstrated the existence of critical regimes in GaAs at elevated temperatures in which the residual ion damage is *extremely* sensitive to both ion flux and substrate temperature,[5] and that, at sufficiently high temperatures, amorphization in GaAs becomes nucleation limited,[6] creating amorphous layers at depths away from the depth of maximum energy deposition. In this paper, we present measurements of the amorphization kinetics of GaAs during irradiation with a variety of ion species. Specifically, we study the threshold conditions for amorphization in GaAs under$\simeq$100 keV boron, carbon, oxygen, silicon, argon, and germanium irradiation at constant ion fluence.

II. EXPERIMENT

Pieces of single-crystal, semi-insulating (100) GaAs were mounted onto a nickel target block with conducting silver paste. The target block contained a resistive heater and a K-type thermocouple. To minimize errors in temperature measurement, consecutive implants were made into adjacent regions on single pieces of GaAs, with at least a 2 mm spacing between the closest edges of each irradiated area. The temperature of the wafer pieces was varied by adjusting the temperature of the entire sample block after each implant, always starting with the highest temperature. In addition, the position and order of the implants on the nickel sample block were varied. The relative accuracy of temperature measurement across a well-bonded wafer is estimated to be $\approx\pm2$ °C as obtained by the reproducibility of damage measurement under conditions where sharp changes in damage with temperature were obtained. Further details of the experimental configuration and procedures are given elsewhere.[6]

Samples were implanted with B, C, O, Si, Ar, or Ge ions at energies of 95 and 100 keV and ion fluxes ranging from 5×10^{11} to $5\times10^{13}\,\mathrm{cm^{-2}\,s^{-1}}$. The irradiations were performed at substrate temperatures from -196–$+120$ °C. After implantation, samples were analyzed by RBS/channeling with 2 MeV He ions, backscattered into detectors at 100° and $\simeq$170° to the incident beam direction. Samples implanted at temperatures near or below room temperature were analyzed immediately ($\lesssim$1 h), or were stored in liquid nitrogen prior to analysis to minimize post-implant annealing at room temperature. Selected samples were analyzed by cross-sectional

 ©2001 The American Physical Society

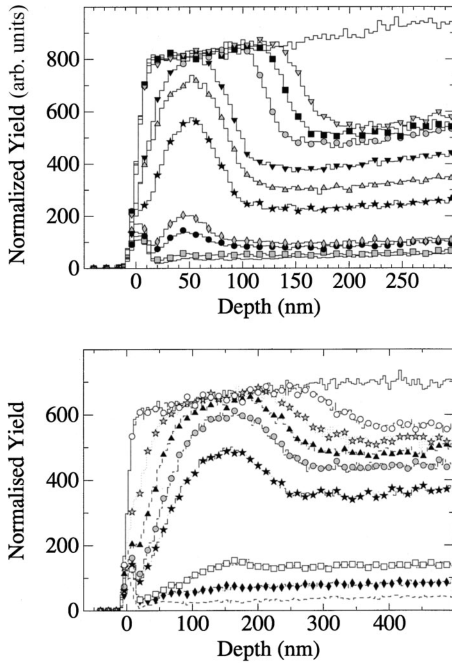

FIG. 1. RBS depth profiles from GaAs irradiated at $\simeq$80 K with (a) 95 keV Si and (b) 100 keV B ions. The Si fluences in (a) are 2.2, 4.3, 4.5, 6.7, 7.7, and $8.6\times10^{13}\,\mathrm{cm}^{-2}$ and 2.2, 4.3, and 8.6 $\times10^{14}\,\mathrm{cm}^{-2}$. The B fluences in (b) are 2×10^{14}, 3×10^{14}, 3.5 $\times10^{14}$, 3.7×10^{14}, 4.2×10^{14}, 5×10^{14}, $1\times10^{15}\,\mathrm{cm}^{-2}$.

transmission electron microscopy (XTEM) at 200 keV to determine the damage microstructure. Sample preparation for XTEM was by mechanical polishing followed by Ar ion milling on a liquid nitrogen cooled stage.

III. RESULTS AND DISCUSSION

A. Defect accumulation and amorphization

The structural damage created by ion irradiation of GaAs at 77 K ($-196\,^\circ$C) is essentially free from dynamic annealing effects during implantation. Figure 1(a) shows RBS depth profiles of GaAs irradiated with 95 keV Si ions at $\simeq$80 K to fluences from $2.2\times10^{13}\,\mathrm{cm}^{-2}$ to $8.6\times10^{14}\,\mathrm{cm}^{-2}$. The "random," or nonaligned profile and the "virgin" profile from unirradiated GaAs are shown as solid lines without symbols. The other profiles with symbols show the typical accumulation of damage with increasing fluence, with an initial increase in the dechanneling level at $2.2\times10^{13}\,\mathrm{cm}^{-2}$ (shaded squares), the appearance of a direct scattering peak at a depth of $\simeq$50 nm at a fluence of $4.3\times10^{13}\,\mathrm{cm}^{-2}$ (solid circles), and the increase in height and width of this peak with increasing fluence until the RBS yield is coincident with the random level from the surface down to a depth of $\simeq$150 nm at $8.6\times10^{14}\,\mathrm{cm}^{-2}$ (shaded inverted triangles), suggesting the formation of a thick amorphous layer. The ion flux was $9.6\times10^{11}\,\mathrm{cm}^{-2}\,\mathrm{s}^{-1}$, but varying the flux by a factor of 5 did not change the damage level, supporting the assertion that dynamic annealing is negligible in GaAs at this temperature.

Figure 1(b) shows a similar evolution of damage for irradiation at $\simeq$77 K with 100 keV ^{11}B ions. For this light ion,

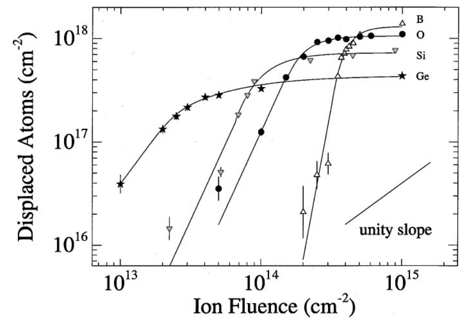

FIG. 2. The areal density of displaced atoms in GaAs as a function of ion fluence for irradiation with 95 keV B, O, Si, and Ge ions at $\simeq$80 K.

the fluences shown are approximately one order of magnitude greater than those for Si ions as shown in Fig. 1(a), ranging from $2\times10^{14}\,\mathrm{cm}^{-2}$ to $1\times10^{15}\,\mathrm{B\,cm}^{-2}$. Because the rates of electronic and nuclear energy loss are considerably smaller for B ions than for Si ions, the damage appears deeper into the crystal, producing a direct scattering peak at a depth of $\simeq$150 nm for a fluence of $3.5\times10^{14}\,\mathrm{B\,cm}^{-2}$ (solid stars). At a fluence of $1\times10^{15}\,\mathrm{B\,cm}^{-2}$ (open circles), the RBS yield is coincident with the random level from the surface down to a depth of $\simeq$300 nm, again suggesting the formation of a thick amorphous layer.

The accumulation of damage may be quantified by extracting the direct scattering contribution from the measured RBS yield. This is achieved by subtracting the dechanneling component, obtained by scaling the dechanneling cross section to match the dechanneling yield beyond the depth of the damage distribution.[7] This gives a depth profile of the number of "displaced atoms" N_d as a function of depth. Figure 2 shows a plot of the integrated damage extracted from RBS data as a function of ion fluence for implantation of $\simeq$100 keV B, O, Si, and Ge ions at $\simeq$80 K. Several features of the plot may be noted. First, the ion fluence which produces a given amount of "damage," measured by RBS, is, of course, strongly dependent upon the ion species, with approximately two and one half orders of magnitude between the lightest and heaviest ions B and Ge. Secondly, the *total* (i.e., integrated) amount of damage *increases* with decreasing atomic number z, due to the greater depth of the damage profile for lighter ions resulting from their lower rates of energy loss. Finally, the rate of damage accumulation with ion fluence, as measured by the slope of the curves, is substantially greater than unity (typically $\approx$ 4.4) for all ion species. This implies that, even at low temperatures, the production of amorphous layers does not occur by a simple accumulation of amorphous zones produced by single ion impacts, but by some cooperative process, involving the interaction of primary defects created by ion impacts with preexisting damage. XTEM investigations of the damage at ion fluences which produce RBS yields below the random level[8] (not shown) show a distribution of small defect clusters, with no evidence for the amorphous phase. However, one must be careful when interpreting the data from samples implanted at low temperatures, since post-implant annealing of low level damage occurs within hours of warming GaAs to room temperature.[8,9]

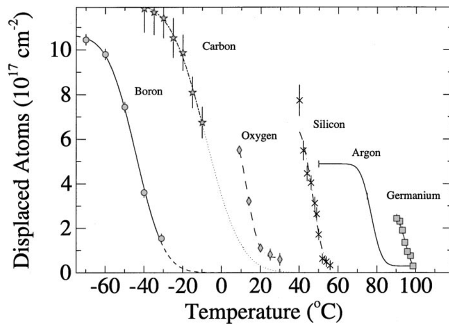

FIG. 3. The areal density of displaced atoms in GaAs as a function of substrate temperature for irradiation of GaAs with $1\times10^{15}\,\mathrm{cm}^{-2}$ of 95 keV B (flux $2.2\times10^{12}\,\mathrm{cm}^{-2}\,\mathrm{s}^{-1}$), C (flux $6.0\times10^{12}\,\mathrm{cm}^{-2}\,\mathrm{s}^{-1}$), O (flux $4.8\times10^{12}\,\mathrm{cm}^{-2}\,\mathrm{s}^{-1}$), Si (flux $4.8\times10^{12}\,\mathrm{cm}^{-2}\,\mathrm{s}^{-1}$), Ar (flux $2.6\times10^{12}\,\mathrm{cm}^{-2}\,\mathrm{s}^{-1}$), and Ga (flux $6.0\times10^{12}\,\mathrm{cm}^{-2}\,\mathrm{s}^{-1}$) ions.

At temperatures above $\simeq$200 K ($-73\,°$C), defects in GaAs become mobile[10] and residual radiation damage will be the result of defect production, trapping and annealing processes. XTEM examination[11] of irradiated samples shows that radiation damage in GaAs first takes the form of isolated defect clusters, presumably by trapping mobile defects. With increasing ion fluence, the size and density of these clusters also increases. At some critical defect density, these clusters may collapse to form the amorphous phase. Once nucleated, the amorphous regions grow rapidly to form a discontinuous amorphous layer. A similar transition may be observed at constant ion fluence by changing the temperature of irradiation. Dynamic annealing during irradiation increases with increasing temperature through thermally activated defect diffusion, dissociation, and annihilation processes. Hence the irradiation conditions that lead to the formation of an amorphous layer at 30 °C only produce defect clusters at 80 °C. However, essentially the same damage morphologies are seen in each case, irrespective of ion species, fluence, flux, and temperature within the parameter space investigated.

It is instructive to observe the phase space of irradiation parameters which defines the amorphization threshold. Figure 3 shows the integrated damage measured by RBS as a function of substrate temperature for irradiation with 100 keV, $1\times10^{15}\,\mathrm{cm}^{-2}$ B, C, O, Si, Ar, and Ge ions at similar ion fluxes (see figure caption for actual values). For each ion, the damage level is essentially constant at low temperatures, then decreases with increasing temperature to a very low level (essentially zero) over a narrow temperature range of $\sim$10 °C. In Fig. 3, only the transition region (region of sharp decrease in damage) for each ion is shown for clarity. As in Fig. 2, the damage at temperatures below the transition increases with decreasing atomic number due to the increasing thickness of damaged crystal. The width of the transition also increases with decreasing atomic number for the same reason: the large energy straggling of light ions means that regions well away from the depth of maximum energy deposition also contribute to the damage profile. XTEM data[8] indicates that the transition region corresponds to a transition from an amorphous layer to small defect clusters. Thus, Fig. 3 demonstrates that the conditions for amorphization exist in

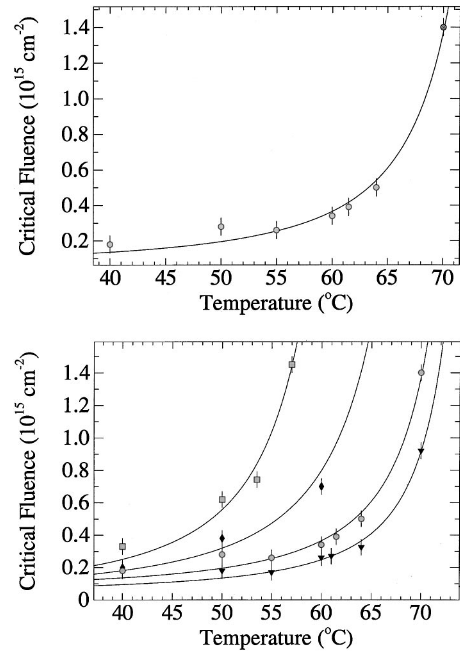

FIG. 4. (a) The ion fluence at which amorphization occurs as a function of substrate temperature for irradiation of GaAs with 95 keV Si ions at a flux of $2.4\times10^{13}\,\mathrm{cm}^{-2}\,\mathrm{s}^{-1}$. (b) As for (a), but for four different ion fluxes, ranging from 6.0×10^{12} to $4.8\times10^{13}\,\mathrm{cm}^{-2}\,\mathrm{s}^{-1}$ by factors of 2. The solid lines are fits to the Morehead and Crowder model (Ref. 12).

well-defined temperature regions, with heavier ions having higher temperature transitions, from $\simeq-40\,°$C for boron, to $\simeq$95 °C for germanium ions. This can be understood qualitatively; for example, heavier ions create more defects per ion, so that a higher temperature may be required to anneal these defects. However, ions of larger atomic number and mass will also generate defects at a higher rate. Physically, the net damage rate is the result of competing defect production, trapping and annealing processes. The defect production rate is proportional to the ion flux in undamaged crystal, so flux is expected to be a key parameter in determining the residual damage.

B. Flux dependence

Figure 4(a) shows the fluence of 95 keV Si ions required to amorphize GaAs as a function of temperature at a flux of $2.4\times10^{13}\,\mathrm{cm}^{-2}\,\mathrm{s}^{-1}$. As the temperature increases, the amorphization fluence rises ever more sharply. It may be said that at sufficiently high temperatures, GaAs "cannot be amorphized." What is meant by this statement is that the amorphization fluence becomes so large ($\gtrsim10^{16}\,\mathrm{cm}^{-2}$), the concentration of implanted ions so high ($\gtrsim7\times10^{20}\,\mathrm{cm}^{-2}$, or >1 at. %), that the irradiated region can no longer be said to be GaAs. As we have shown elsewhere,[6] what actually occurs in this regime is that the crystalline-to-amorphous phase transformation becomes nucleation limited. Under these conditions, nucleation occurs either at the free surface, or at extrinsic dislocations punched out by excess interstitial atoms.

The solid line going through the data points in Fig. 4(a) is a fit to the ubiquitous Morehead and Crowder model[12] of

amorphous layer formation. This model describes a "heterogeneous" model whereby zones of GaAs amorphized directly by single ion impacts accumulate to form a continuous amorphous layer. As others have found, the model is able to fit our data rather well. The fit gives values for the radius $r = 7$ Å of the individual amorphous zones, the annealing activation energy for the shrinkage of the zones $E_a = 0.33$ eV, and the temperature, $T_\infty = 78$ °C at which the amorphization fluence becomes infinite.

Figure 4(b) shows the same data for four values of ion flux, ranging from 6.0×10^{12} to $4.8\times10^{13}\,\mathrm{cm^{-2}\,s^{-1}}$ by factors of 2. Again, the solid lines are fits to the Morehead and Crowder model. Clearly, the ion flux has a dramatic effect on the amorphization of GaAs, with increasing ion flux increasing the temperature (or reducing the fluence) threshold for amorphization. The calculated activation energy for amorphous core annealing more than doubles from 0.16 to 0.33 eV with an increase of ion flux by a factor of 2 from 1.2×10^{13} (diamonds) to $2.4\times10^{13}\,\mathrm{cm^{-2}\,s^{-1}}$ (circles). It is difficult to imagine that this annealing barrier should change so dramatically with such a relatively small increase in ion flux.

The reason for the above behavior is presumably that the underlying assumptions of the Morehead and Crowder model are not applicable to the actual processes occurring during irradiation. We have found[8] that, under our irradiation conditions, amorphous layers are not formed in GaAs by the accumulation of isolated zones formed by single ions, but rather by a collapselike process at defect complexes. Although we can fit our data to this (and other[5]) models and extract values for physical parameters, these values may not be meaningful if the model does not describe the real underlying defect processes. Nevertheless, such models can be useful for estimating the accumulation of "damage," or the irradiation conditions required for amorphization, if these conditions are reproduced.

Because radiation damage is the result of competing defect production, diffusion, trapping, and annealing processes, it is instructive to remove the fluence dependence and examine the relationship between ion flux and substrate temperature, since the former determines the defect production rate, and the latter determines the diffusion, trapping, and annealing rates. When the production and annealing rates are closely balanced, changes in flux and temperature will shift the balance and produce large changes in the resulting defect morphology.[5] These changes can be studied in the hope of elucidating the underlying defect processes.

Figure 5 shows the normalized maximum yield of displaced atoms extracted from BBS damage profiles as a function of substrate temperature for irradiation of GaAs with 95 keV Si ions at ion fluxes of 4.8×10^{12} and $4.8\times10^{13}\,\mathrm{Si\,cm^{-2}\,s^{-1}}$, differing by one order of magnitude. The data show an extremely narrow transition from 100% disorder to almost zero disorder over a temperature range of only ≈6 °C. We denote the temperature of this transition as the "critical temperature," or T_c, corresponding to the threshold conditions for the crystalline to amorphous phase transformation in GaAs. The effect of changing the ion flux by one order of magnitude is to shift the critical temperature by 27 °C.

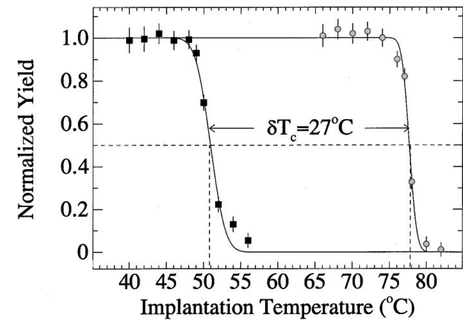

FIG. 5. The normalized maximum yield of displaced GaAs atoms as a function of substrate temperature for implantation of 95 keV Si to a fluence of $1\times10^{15}\,\mathrm{Si\,cm^{-2}}$ at fluxes of 4.8×10^{12} and $4.8\times10^{13}\,\mathrm{Si\,cm^{-2}\,s^{-1}}$. The rapid decrease in residual damage defines a critical temperature T_c for amorphization, as confirmed by XTEM (Ref. 8). The order of magnitude change in ion flux has produced a shift of T_c by 27 °C.

Figure 6 plots the critical temperature T_c defined above as a function of ion flux for irradiation with 95 keV, $1\times10^{15}\,\mathrm{Si\,cm^{-2}}$, illustrating the strong flux effect on amorphization in GaAs. We have also included in this figure one data point (shaded square) derived from the work of Haynes and Holland[3] at a much lower flux (and a slightly lower fluence of $6\times10^{14}\,\mathrm{cm^{-2}}$) than used in the present study. The solid line connecting the critical temperature points separates regions of parameter space defining either conditions for amorphization or retained crystallinity. This flux data is entirely consistent with the temperature and fluence effects shown earlier. Lowering the flux in a regime where dynamic annealing closely balances damage production lowers the damage production rate and can result in the dominance of dynamic annealing and the suppression of amorphization. The critical temperature rises sharply at low ion fluxes, flattening out at higher values. The form of this dependence suggests a thermally activated process. Figure 7 shows a plot of the maximum displacement flux density [i.e., the product of ion flux with the maximum number of atomic displacements per ion per unit length calculated by TRIM (Ref. 13)]

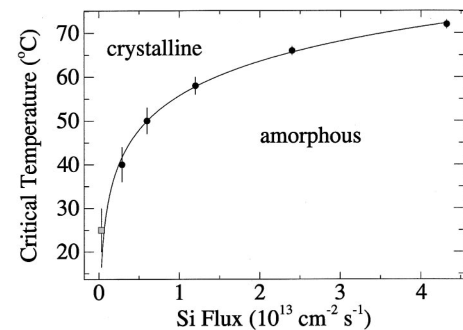

FIG. 6. The critical temperature for amorphization T_c as a function of ion flux for implantation of 95 keV Si to a fluence of $1\times10^{15}\,\mathrm{cm^{-2}}$. The data point shown as a shaded square was derived from the paper of Haynes and Holland[3] for a slightly lower fluence of $6\times10^{14}\,\mathrm{cm^{-2}}$. The solid line separates regions of parameter space defining either conditions for amorphization or retained crystallinity.

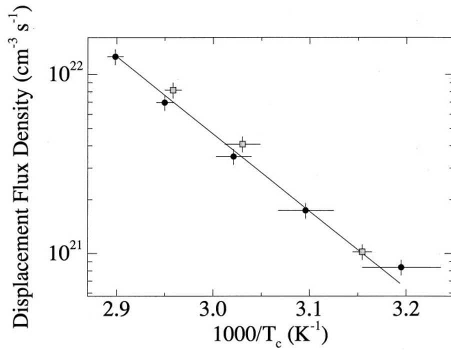

FIG. 7. Displacement rate (i.e., product of ion flux and displacements per ion per unit length from TRIM) versus inverse critical temperature. The data for both 95 keV and 1.5 MeV Si ions is described by a single activation energy of 0.9 ± 0.1 eV.

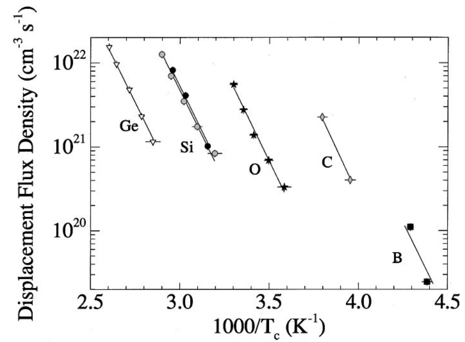

FIG. 9. Displacement flux density as a function of inverse critical temperature for irradiation of GaAs with $1\times10^{15}\,\mathrm{cm}^{-2}$ B, C, O, Si, and Ge ions. The lines connecting the data points for each species all correspond to the same activation energy of 0.9 eV.

for 95 keV Si ions (circles) as a function of inverse critical temperature. The straight line fit to the data indicates a single activation energy with a value of 0.9 ± 0.1 eV. The shaded squares represent the amorphization threshold for irradiation with 1.5 MeV Si ions to the same ion fluence. The fact that the two sets of data coincide demonstrates that the energy of the ions is only important in that the effective flux decreases with increasing ion energy due to energy straggling. It also suggests that beam heating did not appreciably raise the sample temperature for these elevated temperature implants. Similarly, an increase or decrease of the ion fluence by more than a factor of two (not shown) has no apparent effect on the measured activation energy.

Similar data was obtained for other ions. Figure 8 shows a plot of the critical temperature for amorphization as a function of ion flux for irradiation with B, C, O, Si, and Ge ions to the same ion fluence of $1\times10^{15}\,\mathrm{cm}^{-2}$. Each ion has a significantly different range of values for T_c, as we show above in Fig. 3. The shaded band denotes the range of temperatures spanning 20 to 30 °C, which may be loosely described as "room temperature." The figure shows that the amorphization threshold may or may not be within this range, depending on the irradiation conditions. For the fixed fluence of $1\times10^{15}\,\mathrm{cm}^{-2}$ shown here, only low ion fluxes (e.g., $\lesssim2\times10^{12}\,\mathrm{cm}^{-2}\,\mathrm{s}^{-1}$) of Si ions fall within this range, whereas only high ion fluxes (e.g., $\gtrsim1.5\times10^{13}\,\mathrm{cm}^{-2}\,\mathrm{s}^{-1}$) of

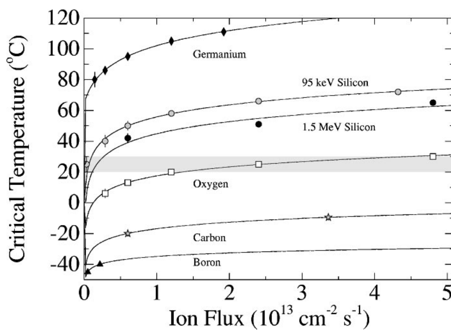

FIG. 8. Critical temperature T_c as a function of ion flux for irradiation of GaAs with B, C, O, Si, and Ge ions. The shaded band denotes the range of temperatures spanning 20 to 30 °C, which may be loosely described as "room temperature."

O ions qualify. Ions with atomic numbers smaller than 7 will never lie within this range, and ions with atomic numbers larger than $\simeq$20 will probably never lie within this range, or only at extremely low ion fluxes. Thus the figure indicates that blanket statements such as "the damage in GaAs is very sensitive to irradiation conditions near room temperature" only apply for certain ion species (e.g., from N to Ar) within certain flux and fluence ranges.

Figure 9 shows a plot of the displacement flux density as a function of inverse critical temperature for several ions. Remarkably, the data for each ion is well described by a straight line with the same slope of 0.9 ± 0.1 eV. This suggests that the amorphization threshold may be determined by a single, thermally activated process with this activation energy. Note, however, that unlike the data for 95 keV and 1.5 MeV Si ions, the data do not lie on a single line, but display a range of critical temperatures, even when producing defects at the same rate, according to TRIM calculations. This suggests that it is not only the raw defect generation rate that determines the critical temperature, but also the density of the collision cascade, as one might expect. Intriguingly, the data does appear to scale[8] with the product of the ion flux and the fourth power of the TRIM displacement rate, which might be expected to apply if fourth order defects (e.g., interacting divacancies) controlled the amorphization process. However, without further supporting evidence, we restrict ourselves to this observation. We speculate that the pathway to amorphization involves the formation of defect complexes which eventually transform locally to the amorphous phase at some critical defect density. Heavier ions may produce these intermediate defect complexes more readily in dense collision cascades. Nevertheless, the single activation energy value suggests that the modifications to this defect structure which lead to the nucleation threshold for the amorphous phase are still limited by a single defect diffusion, trapping, and/or annihilation process.

IV. CONCLUSION

The crystalline-to-amorphous phase transformation in ion-irradiated GaAs has been investigated by XTEM and RBS with ion channeling. The amorphous phase nucleates

locally by a collapselike process at defect complexes when a critical free energy is exceeded to produce discontinuous amorphous layers. The same microstructures of damaged GaAs have been observed for a range of ion species and temperatures from -60–$120\,^{\circ}\mathrm{C}$. The critical relationships between ion flux and substrate temperature which define the threshold conditions for amorphization in GaAs, by irradiation with various ions at constant fluence, have been measured. The threshold conditions for nucleation are shown to be thermally activated, with a single activation energy of $0.9\pm0.1\,\mathrm{eV}$, apparently independent of ion species, energy or fluence. However, the conditions for nucleation lead to a sensitivity to implant conditions in species-dependent temperature ranges. For ion fluences of $\sim10^{15}\,\mathrm{cm}^{-2}$ at typical ion fluxes, the residual damage may be extremely sensitive to implant conditions near room temperature for Si ions. However, this is not generally true for other ion species: the damage created by significantly lighter (e.g., $z<7$) or heavier (e.g., $z>20$) ions at typical ion fluences is only sensitive to implant conditions at temperatures well below or above room temperature, respectively. Despite the independence of the measured activation energy on ion species, the critical temperature for amorphization does not scale linearly with the rate of energy deposition or displacement density, indicating that details of the collision cascade which influence defect quenching, trapping, clustering and annihilation processes determine the pathway to amorphization. We speculate that this results from the difficulty of nucleating or stabilizing the amorphous phase in this material at temperatures where defects are highly mobile, and that nucleation occurs locally at stable defect complexes which are formed more readily in the dense collision cascades created by heavier ions. However, we are not yet able to identify the specific defect limiting process which characterises amorphization and leads to the measured $0.9\pm0.1\,\mathrm{eV}$ activation energy.

[1] W. H. Weisenberger, S. T. Picraux, and F. L. Vook, Radiat. Eff. **9**, 121 (1971).
[2] N. A. G. Ahmed, C. E. Christodoulides, and G. Carter, Radiat. Eff. **52**, 211 (1980).
[3] T. E. Haynes and O. W. Holland, Appl. Phys. Lett. **59**, 452 (1991).
[4] J. M. Poate and J. S. Williams, in *Ion Implantation and Beam Processing*, edited by J. S. Williams and J. M. Poate (Academic Press, Australia), (1984), p. 13.
[5] R. A. Brown and J. S. Williams, J. Appl. Phys. **81**, 7681 (1997).
[6] R. A. Brown and J. S. Williams, Phys. Rev. B **55**, 12 852 (1997).
[7] J. F. Ziegler, J. Appl. Phys. **43**, 2973 (1972).
[8] R. A. Brown, Ph.D. thesis, University of Melbourne, 1995.
[9] F. L. Vook, J. Phys. Soc. Jpn. **18**, 190 (1963).
[10] K. Thommen, Radiat. Eff. **2**, 201 (1970).
[11] R. A. Brown and J. S. Williams (unpublished).
[12] F. F. Morehead and B. L. Crowder, Radiat. Eff. **6**, 27 (1970).
[13] J. P. Biersack and L. G. Haggmark, Nucl. Instrum. Methods **174**, 257 (1980).